

# Optical plasma emission spectroscopy of etching plasmas used in Si-based semiconductor processing

V M Donnelly<sup>1</sup>, M V Malyshev<sup>2</sup>, M Schabel<sup>2</sup>, A Kornblit<sup>2</sup>, W Tai<sup>2</sup>  
I P Herman<sup>3</sup> and N C M Fuller<sup>3</sup>

<sup>1</sup> Department of Chemical Engineering, University of Houston, Houston, TX, USA

<sup>2</sup> Bell Laboratories, Lucent Technologies, Murray Hill, NJ, USA

<sup>3</sup> Columbia University, New York, NY, USA

E-mail: Plasma1356@aol.com

Received 26 September 2001, in final form 3 July 2002

Published 19 August 2002

Online at [stacks.iop.org/PSST/11/A26](http://stacks.iop.org/PSST/11/A26)

## Abstract

Previously published applications of optical emission spectroscopy as a quantitative plasma diagnostic technique are reviewed. By adding traces of rare gases to the plasma, electron temperatures ( $T_e$ ) and relative electron and ion densities can be determined from electron impact-induced optical emission. Excitation from both the ground state and metastable states of the rare gases must be considered. At higher rare gas partial pressures, UV radiation trapping and optical cascading must also be taken into account. Absolute species concentrations (e.g.  $\text{Cl}_2$ ,  $\text{Cl}$ ,  $\text{O}$ , and  $\text{F}$ ) can be derived from their optical emissions, combined with  $T_e$  measurements determined from rare gas optical emission. Examples are given of neutral and ion species density measurements in chlorine, oxygen, and fluorocarbon-containing low-pressure, high charge-density plasmas. Typical results of  $T_e$  measurements are also presented and compared with Langmuir probe measurements.

## 1. Introduction

Collisions of high-energy electrons ( $\sim 5$  to  $\sim 50$  eV) with neutral species create electronically excited neutrals and positive ions in a plasma. These excited species decay and emit light at characteristic wavelengths. This optical emission can be used as a qualitative indicator of the presence of atoms, small molecules, and energetic electrons in the plasma. For example, the optical emission spectrum of a chlorine plasma with traces of the five rare gases (figure 1) contains emissions from  $\text{Cl}_2$ ,  $\text{Cl}$ ,  $\text{Cl}_2^+$ ,  $\text{Cl}^+$  (not shown), Si, and the rare gases. To convert these qualitative observations into quantitative number densities and energy distributions, more information is required.

Quantitative absolute species concentrations can be derived in principle from optical emission intensities, if the mechanism for electron impact can be established, if the electron impact excitation rate constant(s) or cross section(s) for excitation of the emitting state is known, if the electron

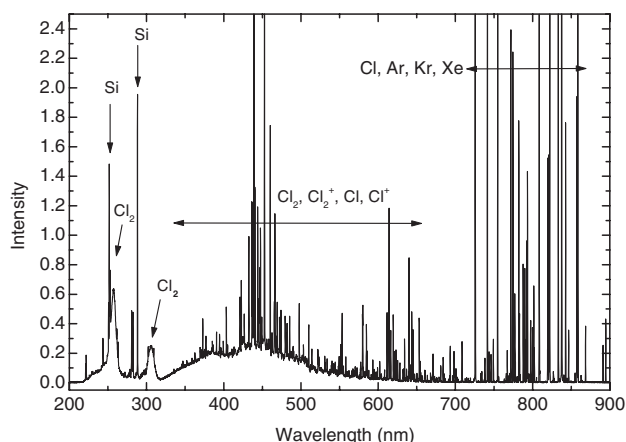


**Figure 1.** Optical emission spectrum of an inductively-coupled chlorine plasma with 1% ea. of the five rare gases, during slow etching of  $\text{SiO}_2$ .

number density and energy distribution (or at least the electron temperature,  $T_e$ ) is known, and if the absolute sensitivity of the spectrometer has been determined. In practice, all of these requirements are rarely met. Specifically, it is usually very difficult to obtain an accurate measure of electron number density and energy distribution at the high energies important for excitation of the emitting species. Obtaining an absolute calibration of the spectrometer sensitivity is also difficult, especially when the transmission of the window on the plasma reactor is decreasing with time due to films deposited from the plasma. Fortunately, there are alternatives to this 'brute-force' approach.

## 2. Determination of plasma electron temperatures by trace rare gases optical emission spectroscopy

Electron temperatures ( $T_e$ ) are commonly measured with a Langmuir probe. In many commercial plasma systems, however, such measurements are difficult or impossible. Often the reactor's walls are coated with insulating materials, making it difficult to obtain a good return path for the Langmuir probe current. Also, concerns with contamination make it undesirable to insert a probe into the plasma. We have avoided these problems with a non-intrusive optical emission technique, using small quantities of the rare gases [1–10]. This trace rare gases optical emission spectroscopy (TRG-OES) method primarily measures the important high-energy tail of the electron energy distribution function (EEDF). Previously we have studied chlorine and oxygen-containing plasmas [1–10]. Very recently, we applied the technique to fluorocarbon ( $C_2F_6$  and  $C_4F_8$ )/Ar plasmas [11].

The electron temperature is obtained as an adjustable parameter in a model that computes the optical emission intensities of selected Ar, Kr, and Xe lines and finds the best match to the experimental measurements. A schematic energy level diagram is shown in figure 2. Electron impact excites rare gas atoms from their ground states to the Paschen 2p levels. These excited levels decay on a short ( $\sim 20$  ns) timescale to one of four levels (two of which are metastable) and emit photons in the red–near-infrared region. Alternatively, electron impact excitation can occur from the ground state to levels above the 2p manifold. These levels also decay on a short timescale, accompanied by emission of a vacuum

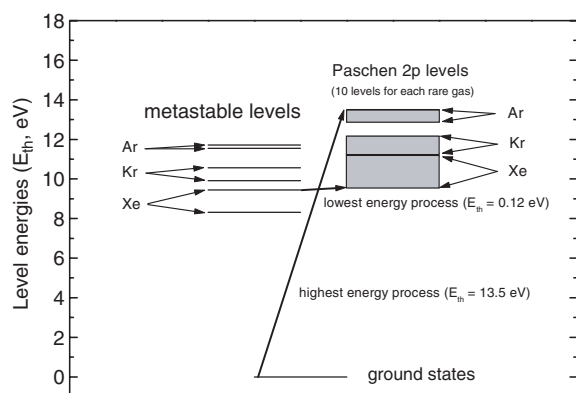


**Figure 2.** Relevant rare gas energy levels and pathways for electron impact excitation.

ultraviolet (VUV) photon (when decaying to the ground state) or a longer wavelength photon when decaying to the 2p levels or higher-lying levels. This cascading mechanism increases the intensity of emission from the 2p levels. At low pressures, this enhancement is part of the electron impact excitation cross section measured in experiments where photons are detected (as opposed to the scattered electrons) [12]. At higher pressures, however, the cascading process becomes enhanced by radiation trapping of the VUV light [12]. The degree of enhancement depends on the rare gas number density, temperature, the size of the plasma, and the viewing geometry. If a given rare gas is present at a very low partial pressure ( $\lesssim 0.2$  mTorr for a typical size processing plasma), then the radiation trapping effect can be ignored. For other cases, such as fluorocarbon plasmas with large additions of Ar, this effect must be included in the model that is used to derive electron temperatures from rare gas emission [11].

Sample  $T_e$  measurements are given in figure 3 for chlorine inductively coupled plasmas [8]. In this case, traces (1% ea.) of the five rare gases were added, hence radiation trapping could be ignored. Also shown are the Langmuir probe measurements of  $T_e$ . At lower pressures and higher powers, where the EEDF tends to be more Maxwellian, the Langmuir probe and TRG-OES values for  $T_e$  are in good agreement. At higher pressures and powers, the EEDF has been observed to have a depleted tail, and the TRG-OES method, which is more sensitive to higher energy electrons, gives lower values for  $T_e$  than does the Langmuir probe, which is more strongly

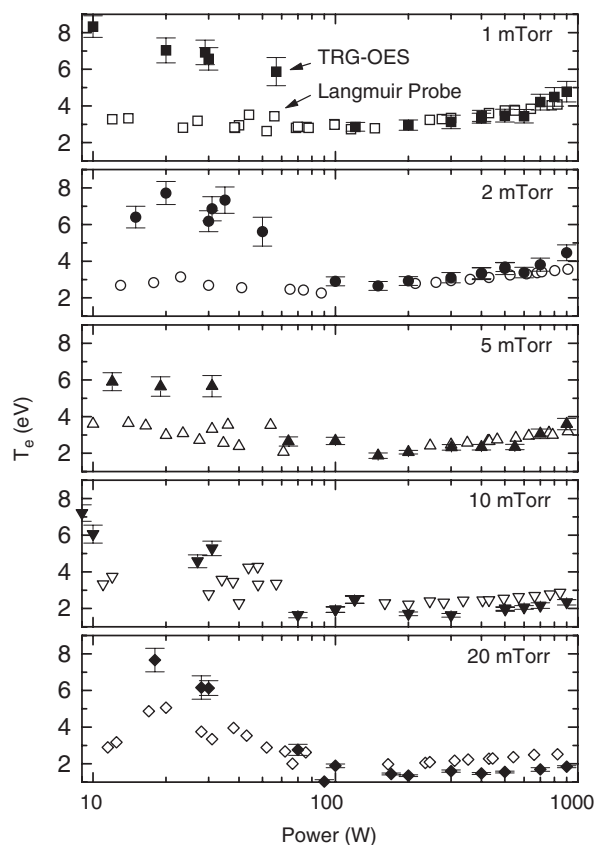


**Figure 3.** Electron temperatures in a  $Cl_2$  inductively-coupled plasma, measured with TRG-OES and a Langmuir probe; from [8].

weighted towards lower energy electrons. In the higher power, inductively coupled mode,  $T_e$  increases with increasing power and decreasing pressure. These effects are well understood from a global model perspective: at lower number densities, the average electron energy must increase to maintain electron impact ionization. In addition to the reduction in number density caused by heating the gas at high powers, the depletion of  $\text{Cl}_2$  and formation of Cl raises the mean ionization potential (IP) of the gas by up to 1.5 eV, causing  $T_e$  to increase, to sustain the ionization process.

In the low-power, capacitively-coupled regime, electron temperatures in the mostly chlorine plasma are higher, especially the TRG-OES values. These high values are believed to be a result of stochastic heating by the oscillating sheaths. This leads to an enhanced high-energy tail. This effect is sensed more strongly by the TRG-OES method because at low plasma densities emission is overwhelmingly excited by high-energy electron impact from the ground states, and not through the metastable levels that are present at very low relative concentrations.

An example of electron temperatures in  $\text{C}_2\text{F}_6/\text{C}_4\text{F}_8$ /carrier rare gases (Ar and/or Ne)/trace rare gases (0.8% ea. of He, Ne, Ar, Kr, Xe) plasmas are reproduced in figure 4 [11]. In this experiment, the major carrier gas was a mixture of Ne and Ar. The fraction of Ne was varied while the total flow of Ar plus Ne was kept constant.  $T_e$  was evaluated by TRG-OES in two ways. First, Ar, Kr, and Xe emission was used and the contribution to Ar emission due to radiation-trapping-induced cascading was taken into account (except for the 100% Ne carrier gas case), as described in more detail elsewhere. Second, Ar emission was not included in the analysis, avoiding the complications from high-pressure cascading in Ar. The two methods are in good agreement, supporting the corrections made for cascading at high Ar pressures.

Figure 4 reveals that  $T_e$  in the fluorocarbon/rare gas plasma increases as a function of the fraction of Ne in the carrier gas. This can be understood in terms of the difficulty in ionizing

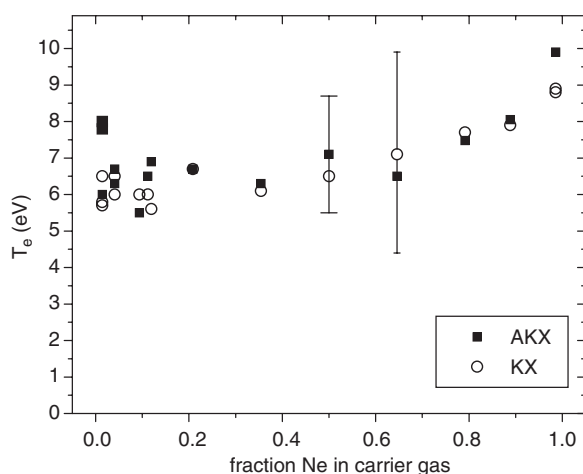


**Figure 4.**  $T_e$  for a (Ar,Ne)/ $\text{C}_2\text{F}_6/\text{C}_4\text{F}_8$ /(equi-mixture of He/Ne/Ar/Kr/Xe) plasma at 95/12/12/7 sccm and 10 mTorr. The fraction of Ne in the carrier gas is varied, showing that for addition of Ne to Ar,  $T_e$  first remains constant and then increases. Source power = 2000 W, bias power = 1000 W. AKX: Ar, Kr, and Xe emission lines were used in the determination of  $T_e$ . KX: Ar and Kr lines were used in the determination of  $T_e$ ; from [11].

Ne (IP = 21.6 eV) vs Ar (IP = 15.8 eV). For comparison, at 10 mTorr and 1000 K (the temperature estimated from  $\text{N}_2$  rotational spectroscopy), a global model predicts  $T_e$  values of 3.2 and 8.1 eV for pure Ar and Ne plasmas, respectively. The observed values are higher, perhaps suggesting additional electron heating from the very high (1000 W) substrate bias power. This would result in a higher ‘temperature’ in the high-energy tail of the electron energy distribution, especially when observations are made close to the biased electrode, as in the present study.

### 3. Species concentrations by advanced actinometry

#### 3.1. Neutral species

Emission features such as the  $\text{Cl}_2$  band at 305 nm and Cl-atom emission (figure 1) can be converted into absolute number densities by dividing these emission intensities by those from the appropriate rare gas at a similar energy. This actinometry method was first reported by Coburn and Chen to measure F-atoms in a  $\text{CF}_4/\text{O}_2$  plasma [13], and has since been widely used by Walkup *et al* [14], d’Agostino *et al* [15], Booth *et al* [16], and many others (see [17]). Recently we used this method, with further refinements to take into account contributions to the rare gas emission from metastables and changes in the actinometry proportionality constants due to changes in  $T_e$  and pumping speeds, and applied it to obtain absolute Cl and  $\text{Cl}_2$  densities in a  $\text{Cl}_2$  plasma [18, 19], O-atom densities in an  $\text{O}_2$  plasma [10], and F-atom densities in a  $\text{C}_2\text{F}_6$ ,  $\text{C}_4\text{F}_8$ , Ar/Ne plasma [11].

Sample measurements of Cl and  $\text{Cl}_2$  number densities in chlorine inductively coupled plasmas are shown in figure 5 as a function of pressure and power [19]. These are measurements of line-averaged number densities, weighted in proportion to the emission intensity, and therefore are characteristic of the high-density region of the plasma.  $\text{Cl}_2$  number densities are obtained from  $\text{Cl}_2$  emission, normalized to Xe emission. Corrections are made for differences in pumping speeds of  $\text{Cl}_2$  and Xe. Xe emission is also corrected for the fraction of emission that is due to electron impact excitation from Xe metastable levels. The proportionality constant needed to convert  $\text{Cl}_2$ -to-Xe emission ratios to absolute  $\text{Cl}_2$ -to-Xe number density ratios is obtained from an extrapolation of the emission ratio to zero power, where the  $\text{Cl}_2$ -to-Xe number density ratio is known from the flow rate ratio and the relative pumping speeds. This proportionality constant is independent of  $T_e$  between  $\sim 1.5$  and 5 eV. A similar analysis is performed to convert the Cl-to-Xe emission ratio to absolute Cl-to-Xe number density ratios. In this case, the proportionality constant is obtained at high powers, where  $\text{Cl}_2$  is shown to be largely dissociated. At low powers, Cl emission is corrected for the fraction of emission that arises from dissociative excitation of  $\text{Cl}_2$ . Finally, absolute number densities are obtained from gas temperature measurements, carried out by  $\text{N}_2$  rotational emission spectroscopy [2].

Figure 5 shows that at very low powers, very little dissociation of  $\text{Cl}_2$  occurs and the  $\text{Cl}_2$  number density is at a value equal to that computed from the pressure and temperature (essentially room temperature). As the plasma switches to the inductive mode at higher powers,  $\text{Cl}_2$  is efficiently

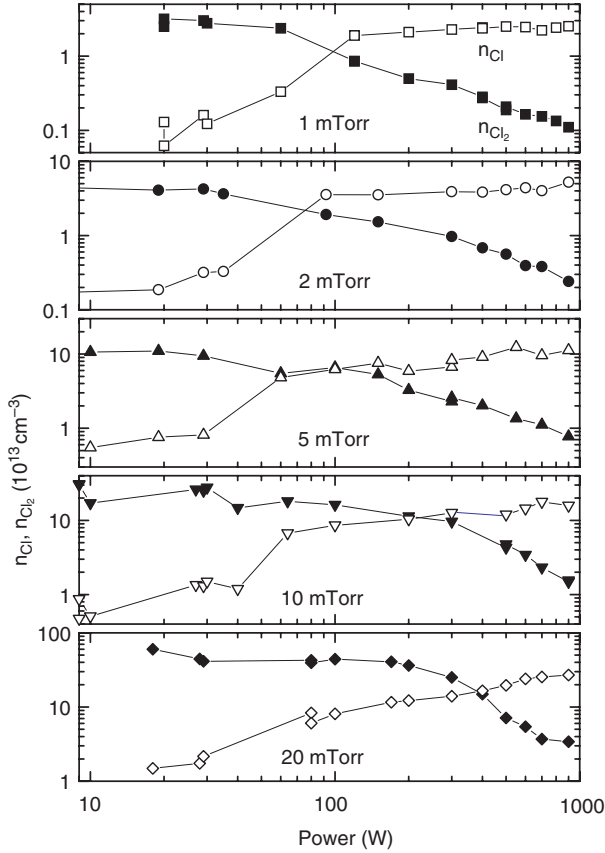


**Figure 5.**  $\text{Cl}_2$  and Cl number densities in a chlorine ICP; from [19].

dissociated and the Cl atom density rises steadily. At the highest powers, the  $\text{Cl}_2$  is largely dissociated, especially at low pressures.

Absolute O atom densities in an oxygen/1% Ar plasma were also obtained previously in the same plasma reactor [10]. In this case, Ar emission (750.4 nm) from the  $2p_1$  level provides a better energy match to the O 844.6 nm emission. While the cross sections for these  $\text{Ar}^{12}$  and O emissions [20, 21] have been measured, at even moderate ( $\sim 5 \times 10^{12} \text{ cm}^{-3}$ ) number densities, trapping of the VUV radiation from higher levels provides the main pathway for excitation of 844.6 nm O atom emission. Consequently, the cross sections for excitation of these higher lying levels can be used to obtain an absolute proportionality constant. To compute the total electron impact excitation rate for the  $3p^3P$  state responsible for the 844.6 nm emission, cascade transitions from higher levels of the triplet manifold (mainly ns ( $n \geq 4$ ), np ( $n \geq 4$ ), nd ( $n \geq 3$ ), and  $3s'$ ) must also be considered. All of these levels can undergo transitions to either the  $3p^3P$  level, accompanied by the emission of a visible to near-infrared photon, or to the ground state, resulting in emission of a VUV photon. At the O atom number densities above  $\sim 5 \times 10^{12} \text{ cm}^{-3}$ , the VUV radiation from excited states above the  $3p^3P$  level, populated by electron impact, cannot escape the plasma and these higher levels are repeatedly excited until they decay to the  $3p^3P$  level. The rate constants computed from the sum of these cross sections, presented in [10], show that the total excitation rate that includes cascade contributions to O atom emission at 844.6 nm is about three times the direct excitation rate.

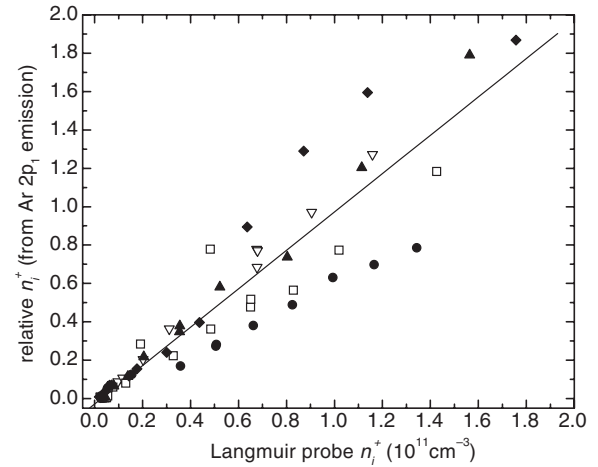


**Figure 6.** Relative positive ion densities in chlorine, trace rare gases plasmas determined from  $\text{Ar}(2p_1)$  optical emission as a function of total positive ion density measured with the Langmuir probe. Total pressures were 1 ( $\bullet$ ), 2 ( $\square$ ), 5 ( $\blacktriangle$ ), 10 ( $\nabla$ ), and 20 ( $\blacklozenge$ ) mTorr. The solid line is a linear least squares fit to all of the data; from [22].

### 3.2. Charged species

Emission from trace rare gases can be used to estimate relative electron densities, and as recently shown [22], total positive ion densities. While quantitative measurements of relative electron densities are complicated by deviations of the EEDF from a pure Maxwellian, determinations of total positive ion densities do not depend strongly on the shape of the EEDF. It can be shown [22] that the positive ion density (mostly  $\text{Cl}^+$ ) in a  $\text{Cl}_2/\text{trace Ar}$  plasma is related to the Ar emission intensity ( $I_{\text{Ar}}$ ) by

$$n_{\text{Cl}}^+ = \frac{c I_{\text{Ar}} k_{\text{Cl}}^{\text{iz}} V}{k_{\text{Ar}} v_{\text{B,Cl}^+} A_{\text{eff,Cl}^+}} \quad (1)$$

where  $c$  is a proportionality constant,  $k_{\text{Cl}}^{\text{iz}}$  is the electron impact ionization rate constant for  $\text{Cl}^+$  from Cl,  $k_{\text{Ar}}$  is the rate constant for excitation of Ar 750.4 nm emission,  $V$  and  $A_{\text{eff,Cl}^+}$  are the plasma volume and effective area, and  $v_{\text{B,Cl}^+}$  is the  $\text{Cl}^+$  Bohm velocity. This method uses the measured Ar emission intensity to estimate the  $\text{Cl}^+$  formation rate and global modelling to determine the  $\text{Cl}^+$  destruction rate. Relative  $\text{Cl}^+$  densities are plotted in figure 6 vs positive ion densities measured with a Langmuir probe [22]. Within a factor of  $\pm 2$ , the relative ion densities measured by emission spectroscopy agree with those measured with the Langmuir probe over a range of powers and pressures. Given the uncertainty in Langmuir probe measurements of ion densities (roughly a factor of 2), this is considered good agreement.

Emission from excited ions can in some cases be shown to be due to electron impact excitation from the ground state of the ion, and not by the higher energy, single electron impact excitation from the ground state neutral. In these cases, Ne actinometry can be used to monitor relative concentrations of ground state ions with excited states that have energies similar to that of Ne ( $2p_1$ ). Measurements of relative concentrations of  $\text{Cl}^+$  and  $\text{Ar}^+$  in  $\text{Cl}_2/\text{Ar}$  plasmas have recently been reported, using this method [23]. In such an analysis, the  $T_e$ -dependence of the proportionality constant must also be taken into account.

Finally, negative ion ( $\text{Cl}^-$ ) densities can also be measured by emission spectroscopy [24]. In this case the reaction



leads to the formation of  $\text{Cl}_2^*$ , which emits in the visible and ultraviolet. This emission can be detected in the afterglow of pulsed plasmas, after the competing electron impact emission has decayed.

#### 4. Summary

Several examples have been given of the use of advanced optical emission spectroscopy as a quantitative plasma diagnostic technique. Small amounts of the five rare gases are added to the plasma. Electron impact-induced emission from these species can be analysed to obtain the plasma electron temperature, as well as relative electron and positive ion densities. A complete analysis involves modelling excitation from both the ground state and metastable states of the rare gases. Differences in pumping speeds of the different species must be considered, and optical cascading caused by UV radiation trapping must also be taken into account. Absolute neutral number densities for important species commonly found in Si etching plasmas ( $\text{Cl}_2$ ,  $\text{Cl}$ ,  $\text{O}$ , and  $\text{F}$ ) can be determined from advanced actinometry. Absolute proportionality constants and their  $T_e$ -dependences can be obtained from reliable electron impact excitation cross sections, or derived from plasma experiments carried out under conditions where the absolute concentrations of these species is known. We have applied these methods to various types of high-density, low-pressure chlorine-, oxygen-, and fluorocarbon-based discharges. When conditions and reactor configurations allow, these methods were compared with conventional Langmuir probe measurements. In these instances, the agreement between optical and probe measurements was quite good. Consequently, these optical methods can be used with confidence in situations where Langmuir probe analysis is difficult or impossible.

#### References

- [1] Donnelly V M, Malyshev M V, Kornblit A, Ciampa N A, Colonell J I and Lee J T C 1998 *Japan. J. Appl. Phys.* **37** 2388–93
- [2] Donnelly V M and Malyshev M V 2000 *Appl. Phys. Lett.* **77** 2467
- [3] Malyshev M V and Donnelly V M 1997 *J. Vac. Sci. Technol. A* **15** 550
- [4] Malyshev M V, Donnelly V M, Kornblit A and Ciampa N A 1998 *J. Appl. Phys.* **84** 137
- [5] Malyshev M V, Donnelly V M and Samukawa S 1998 *J. Appl. Phys.* **84** 1222
- [6] Malyshev M V 1999 *PhD Thesis* Princeton University
- [7] Malyshev M V and Donnelly V M 1999 *Phys. Rev. E* **60** 6016
- [8] Malyshev M V and Donnelly V M 2000 *J. Appl. Phys.* **87** 1642
- [9] Malyshev M V, Donnelly V M, Downey S W, Colonell J I and Layadi N 2000 *J. Vac. Sci. Technol. A* **18** 849
- [10] Fuller N C M, Malyshev M V, Donnelly V M and Herman I P 2000 *Plasma Sources Sci. Technol.* **9** 116
- [11] Schabel M, Donnelly V M, Kornblit A and Tai W 2002 *J. Vac. Sci. Technol. A* **20** 555
- [12] Chilton J E, Boffard J B, Schappe R S and Lin C C 1998 *Phys. Rev. A* **57** 267
- [13] Coburn J W and Chen M 1980 *J. Appl. Phys.* **51** 3134
- [14] Walkup R E, Saenger K L and Selwyn G S 1986 *J. Chem. Phys.* **84** 2668
- [15] d'Agostino R, Cramarossa F, Benedictis S D, Fracassi F, Laska L and Masek K 1985 *Plasma Chem. Plasma Process.* **5** 239
- [16] Booth J P, Joubert O, Pelleteir J and Sadeghi N 1991 *J. Appl. Phys.* **69** 618
- [17] Herman I P 1996 *Optical Diagnostics for Thin Film Processing* (San Diego: Academic)
- [18] Donnelly V M 1996 *J. Vac. Sci. Technol. A* **14** 1076
- [19] Malyshev M V and Donnelly V M 2000 *J. Appl. Phys.* **88** 6207
- [20] Laher R R and Gilmore F R 1990 *J. Phys. Chem. Ref. Data.* **19** 277
- [21] Itikawa Y, Ichimura A, Onda K, Sakimoto K, Takayanagi K, Hatano Y, Hayashi M, Nishimura H and Tsurubuchi S 1989 *J. Phys. Chem. Ref. Data.* **18** 23
- [22] Malyshev M V and Donnelly V M 2001 *J. Appl. Phys.* **90** 1130
- [23] Fuller N C M, Donnelly V M and Herman I P 2001 *J. Appl. Phys.* **90** 3182
- [24] Donnelly V M and Malyshev M V 2001 unpublished data